Journal of the Earth & Space Physics. Vol. 35, No. 1, 2009, P. 17-31

Gravity field implied density modeling of topography, for precise determination of the geoid

Najafi-Alamdari, M[1*]., Sedighi, M[2]. and Tabatabaie, S. H[3].

[1]*Associate Professor, Faculty of Geodesy and Geomatics Engineering, K.N.Toosi University of Technology, Tehran, Iran*
[2]*Senior technical staff, National Cartographic Center (NCC), Tehran, Iran*
[3]*Land seismic manager, National Iran Oil Company (NIOC), Exploration management Dept., Tehran, Iran*

(Received: 24 May 2008 , Accepted: 23 Sep 2008)

Abstract

Precise determination of the geoid using the Stokes-Helmert approach requires a density distribution model within the topography. The model is used for precise evaluation of topographical indirect effects on gravity and potential applied in transforming between the real and the Helmert spaces. The range of mass density variation within the topography is between 1000 and 3100 kg.m^{-3}. Assigning the global average value of $\rho_{\circ} = 2670$ kg.m^{-3} at a point, instead of its real point value, may cause errors of decimeter magnitude in the geoid determination. A regional-local gravity anomaly separation technique using Bouguer gravity anomaly (BA) along with the Free air gravity Anomaly (FA) in the region of Iran are used to estimate the local topographical effect on gravity from the observed anomalies after eliminating the non-density origin long wavelength including isostatic features into the observed BA. A Global Geopotential Model (GGM) is also used to eliminate the deep sited density-origin long wavelength features from the observed anomalies as well. Then, the power spectral analysis, apparent density mapping, and forward modeling techniques are used to convert the local topographical effect on gravity into the corresponding 3-D density model (GRADEN) model in the region. The model showed thorough correlation with the superficial geological density (GEODEN) model at the surface level, provided that the reliable digitization of the model is in order. The GRADEN model minus the constant density demonstrates contributions up to a meter in mountainous areas and 7cm in the RMS scale to the geoid in the region.

Key words: Geoid, Bouguer anomaly, Regional local separation, Stokes-Helmert, Geopotential model

تعیین دقیق ژئوئید برای مدل چگالی به‌دست آمده از میدان ثقل زمین

مهدی نجفی‌علمداری[۱]، مرتضی صدیقی[۲] و سیدهاشم طباطبایی[۳]

[۱] *دانشیار، دانشکده مهندسی نقشه‌برداری، دانشگاه صنعتی خواجه‌نصیرالدین طوسی، تهران، ایران*
[۲] *کارشناس ارشد سازمان نقشه‌برداری کشور، تهران، ایران*
[۳] *مدیر عملیات لرزه‌نگاری شرکت ملی نفت ایران*

(دریافت: ۸۷/۳/۴، پذیرش نهایی: ۸۷/۷/۲)

چکیده

در تعیین دقیق ژئوئید به روش استوکس- هلمرت، به مدل توزیع چگالی برای توپوگرافی زمین نیاز است. مدل چگالی توپوگرافی برای تعیین دقیق اثرات توپوگرافی روی شتاب ثقل و پتانسیل و تبدیل بی‌هنجاری (آنامولی) جاذبه مشاهداتی (فضای واقعی) به بی‌هنجاری هلمرت (فضای هلمرت) به‌کار می‌رود. مقدار عددی چگالی در سطح زمین بین ۱ تا ۱ر۳ (gcm^{-3}) متغیر است ولی در بیشتر موارد از

*Corresponding author: Tel: 021-44216386 Fax: 021-88786213 E-mail: mnajalm@yahoo.com

مقدار متوسط ۲/۶۷ گرم بر سانتی‌متر مکعب برای تعیین ژئوئید مورد قرار می‌گیرد که موجب خطا در محاسبه ارتفاع ژئوئید در حدود دسی‌متر می‌شود.

برای تعیین چگالی توپوگرافی، ابتدا اثرات طول موج‌های بلند موجود در بی‌هنجاری جاذبه بوگه ناشی از بی‌هنجاری‌های چگالی واقع در اعماق و دیگر اثرات طول موج بلند نظیر اثر ایزوستاسی و لایه‌های سبک با گستره وسیع احتمالی در منتل بالایی و عوارض سبک ساختارهای زمین‌شناسی با گستره وسیع احتمالی منطقه‌ای را با استفاده از مفاهیم فیزیکی و در مقایسه بی‌هنجاری جاذبه بوگه با بی‌هنجاری جاذبه هوای آزاد در منطقه حذف می‌کنیم و سپس با استفاده از مدل‌های جهانی ژئوپتانسیل، بی‌هنجاری باقی‌مانده محلی را جدا می‌سازیم. با استفاده از آنالیز طیفی و به‌کارگیری فیلترهای متفاوت، این جداسازی را ادامه می‌دهیم و آناملی‌های جدا شده را منتسب به اعماق متفاوت نسبت می‌دهیم و مدل سه‌بعدی پوسته (تا عمق حدود ۲۰ کیلومتر) را ایجاد می‌کنیم. در روندی تکراری و با کمک روش معکوس، مدل چگالی را تصحیح می‌کنیم، یعنی مقدار تفاوت جواب مدل با مشاهدات را به حد قابل قبولی کاهش می‌دهیم.

میزان اثر بی‌هنجاری چگالی در ارتفاع ژئوئید حداقل و حداکثر ۷۳- و ۱۰۳ سانتی‌متر با انحراف معیار و RMS به ترتیب ۷ و ۸ سانتی‌متر است. با توجه به اعداد به‌دست آمده می‌توان نتیجه گرفت که برای تعیین ژئوئید دقیق اطلاع از میزان چگالی واقعی توپوگرافی لازم است.

واژه‌های کلیدی: ژئوئید، روش استوکس- هلمرت، بی‌هنجاری بوگه، مدل‌های جهانی ژئوپتانسیل، جداسازی بی‌هنجاری جاذبه، مدل‌سازی سه‌بعدی چگالی

1 INTRODUCTION

Precise determination of the geoid requires the density of topography above the geoid to be known. In the Stokes-Helmert method, (Vaníček and Martinec, 1994; Martinec, 1998; Vaníček et al. 1999), however, it is argued that a knowledge of topographical density variation in the lateral direction good to about 5 percent is enough to compute a geoid accurate to a few centimeters. There have been several attempts on evaluating the contribution of lateral mass density anomaly contrast (into the topography) towards the geoidal height by, e.g., Tziavos et al. (1996); Kuhn (2001); Huang et al. (2001); Tziavos and Featherstone (2001). They showed that the contribution or the total effect of the lateral mass density distribution reaches up to 5 centimeters or more in Australia and in the Canadian Rocky Mountains. The effect of lateral mass density anomaly contrast on the gravity itself could reach up to +/-10 mGal on average (Huang et al. 2001; Tziavos and Featherstone, 2001).

A conceivable source of information to investigate the mass density contents of topography is in the near surface gravity field of the Earth. A reliable global solution of gravity potential field known as a Global Geopotential Model (GGM), e.g., EGM96 and EIGEN models, (Lemoine et al. (1998); http://www.gfz-potsdam.de/pb1/op/grace/results/), derived from geodetic satellites orbit analysis, could be used to determine the long wavelengths features of the gravity field emanating from the deep sited density anomalies inside the Earth. The model is expressed in a finite series of spherical harmonics. The series is terminated to a certain degree and order harmonic terms. Hence, it could provide only the long wavelength information of the gravity field either of density or non-density origins. A GGM could be used to develop long wavelength Bouguer gravity Anomaly (BA) up to a selected harmonic (cutoff) degree for a region. For this, the long wavelength topographical effect on potential derived from a Digital Topographical Model (DTM) developed into the long wavelength spherical harmonics has to be subtracted from the GGM (Vaníček et al. 1995). The so determined BA would contain only the long wavelength features of the anomaly, i.e., the features containing information from deep sited density anomalies and any other long wavelength features produced by sources such as, e.g., broad low density upper mantel, isostatic equilibrium of the crust, subsurface broad features density anomalies, etc. It is worth mentioning here that, the long wavelength features of BA derived from GGM and DTM are more reliable than those determined by local or regional surveyed gravity data, i.e., the observed BA on the surface of the earth in a region are reliable only on the short wavelengths. Hence, the short wavelengths isolated (filtered) from the observed data by a GGM considering the reasonable cutoff degree in the GGM would provide the reliable short wavelengths of the anomaly.

2 INTERPREATION OF BOUGURE ANOMALY

The BA by its standard definition can be interpreted as an anomaly representing an "Earth" with no topography above the geoid. In the standard approach of constructing a BA model, the gravity attraction of only a model topography with the average and constant density of $\rho_{\circ} = 2670$ kg.m^{-3}, is computationally removed from the observed gravity, leaving a BA sensitive not only to the density anomaly underneath the geoid but to the removed real lateral density anomaly distribution above the geoid as well. Computationally removing the topography above the geoid violates the isostatic equilibrium of the crust in the gravity field of the Earth. The violation is then reflected in the so constructed BA. Hence, in addition to above mentioned variations, the BA would also be affected by the isostasy either of Airy or Pratt shapes in a region. Since the isostasy varies regionally, the effect on the BA would also be of a regional extent too, i.e., the BA is systematically negative in mountainous regions and positive over seas. Contrary to this, in constructing Free Air gravity Anomaly (FA) the topography is not touched, i.e., the isostatic equilibrium of the crust is not violated, hence, the anomaly is not affected by the isostasy any way. In places where the FA are zero or close to zero the isostatic equilibrium of the crust is complete and its gravitational effect is seen in the BA of the same places. Subba Rao (1996) introduced the zero free air anomaly concept to estimate the effect of isostasy in the BA. There may also be another effect of regional extent and mostly negative on BA arising from a possible broad low density upper mantel (Singh et al. 2003 and Mishra et al. 2004). There may be also some irregularities in BA as well. For instance, a vast subsurface located geological formation of low density could cause a long wavelength negative component in BA (Singh et al. 2003). There are other sources affecting BA in a similar fashion making the density interpretation non-unique, i.e., many distributions of density anomalies at different depths can be used to describe the same gravity anomaly.

Other than those mentioned above, there is however a physical fact that the deep sited density anomalies contribute towards the long wave-length part of BA and subsurface density anomalies contribute towards the short wavelength part of BA. There is, however, an approximate relation between the depth of density anomaly and the corresponding wave number in the BA spectrum is given by Featherstone (1997) as

$$Z_n = \frac{R}{n-1}, \tag{1}$$

where Z_n is the depth, *n* is the wave number, and R is the mean radius of the Earth.

3 LOCAL BOUGUER GRAVITY ANOMALY PREDICTION

For the local (characteristically short wavelengths) gravity anomaly estimation in a region, the observed BAs have to be cleaned for the long wavelength effects of either density origin or the others mentioned in the preceding section. The BAs are first corrected for the two well known and possibly existing long wavelengths effects, usually arising with minus signs, i.e., the effects originated from a) broad low density upper mantel b) isostatic shape of the crust.

The first effect exists also in the FA model of the region, while the FA does not contain the second effect as was explained in the introduction. Considering the model anomalies BA and FA determined at a point P on the earth as

$$FA(P) = g_P - \left(\frac{\partial g}{\partial H}\right)^{FA} H^O - \gamma_0, \tag{2}$$

$$BA(P) = g_P - \left(\frac{\partial g}{\partial H}\right)^{BA} H^O - \gamma_0, \tag{3}$$

where g_P is the observed gravity at a point P, γ_0 is the normal gravity on the normal ellipsoid, $\left(\frac{\partial g}{\partial H}\right)^{FA}$ and $\left(\frac{\partial g}{\partial H}\right)^{BA}$ are the vertical gradient of gravity in the FA and BA models respectively, H^O is the orthometric height of the point P. The vertical gradient of gravity in the BA model is itself the sum of two gradients of FA and the topographical gradient as

$$\left(\frac{\partial g}{\partial H}\right)^{BA} = \left(\frac{\partial g}{\partial H}\right)^{FA} + \left(\frac{\partial g}{\partial H}\right)^{T}. \tag{4}$$

Substituting equation (4) into equation (3) and comparing the resulting equation with Equation (2) yields

$$BA(P) - FA(P) = -\left(\frac{\partial g}{\partial H}\right)^{T} H^O = -\delta g^T(P). \tag{5}$$

where $\delta g^T(P)$ is the gravitational attraction of topography evaluated at the point P. On the mountains, δg^T attains positive values. Then the minus sign on the right hand side of equation (5) does confirm the negative isostatic bias of the BA in the mountainous region. Differencing the two anomalies (equation 5) in a region, does automatically eliminate the first effect if it exists, but the second effect (the isostatic effect) remains untouched since the FA is not affected by the isostasy. The isostatic effect is true and available in BA where FA is already zero (Subba Rao, 1996). A low degree 2-D algebraic surface is fitted (in the least-squares sense) to the BAs at the points with zero FA in a region to approximate the isostatic effect. Calling the surface or the model by ISOSTA, one can then remove the isostatic effect together with the first effect from the observed BAs at the point P through

$$\mathrm{BAR}(P) = \mathrm{BA}(P) - \mathrm{FA}(P) - \mathrm{ISOSTA}(P), \quad (6)$$

where BAR(P) is the remainder or the residual BA after the two long wavelength effects are removed. Now, the BAR(P) obtained from equation (6) after it is multiplied by minus sign will be the anomaly indicating the residual gravity effect of topography:

$$\delta g^T(\text{residual}) = -\mathrm{BAR}. \quad (7)$$

The residual anomaly still contains both long and short wavelength components of only the density origin due to the regional (deep sited) and local (subsurface) density anomalies inside the topography. Figure 1 shows the map of complete BA in Iran. By the complete BA it we mean that both the Bouguer plate and the roughness effects of topography on gravity, i.e., $\delta g^T(P)$, have been considered using equation (3.33) in Martinec (1998). The BAs shown in the figure are based on the gravity observations by the National Cartographic Center of Iran (NCC), National Iran Oil Company (NIOC) and all gravity data available from BGI (Bureau Gravimetrique Internationale) in the region and also $30'' \times 30''$ SRTM (Shuttle Radar Topography Mission), (http://edcsns17. usgs.gov/srtmbil/index.html) digital terrain model of topography. Figure 2 is the map of $\mathrm{BA}(P) - \mathrm{FA}(P)$, equation (5), in Iran. Figure 3 shows the map of ISOSTA determined as was explained above. In the ISOSTA map, i.e., the regional component of BA, it can be seen that the isostatic equilibrium has already taken place under the Zagros Mountain chain (North-West to South direction) while only a little or no equilibrium has yet occurred in the geological time under the Alborz mountain chain (West-East direction). Figure 4 shows the map of $\delta g^T(\text{residual})$, equation (7), in Iran.

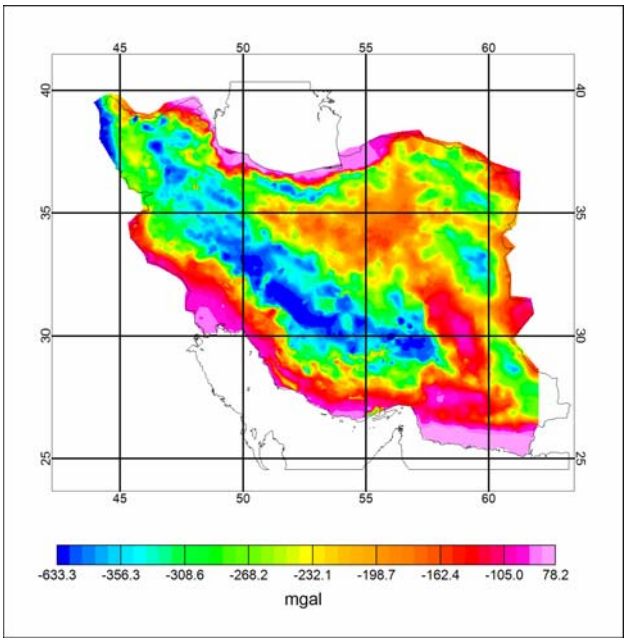

Figure 1. The map of complete BA in Iran.

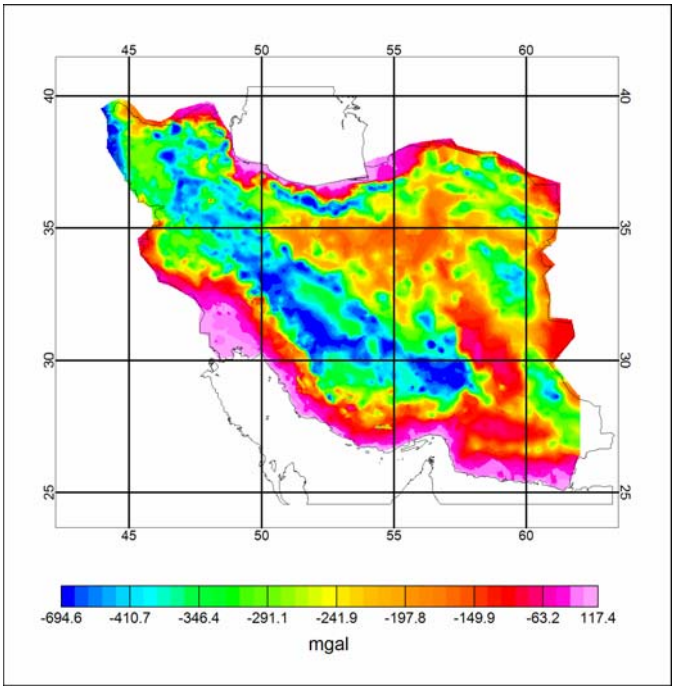

Figure 2. The map of $BA - FA$, equation (5).

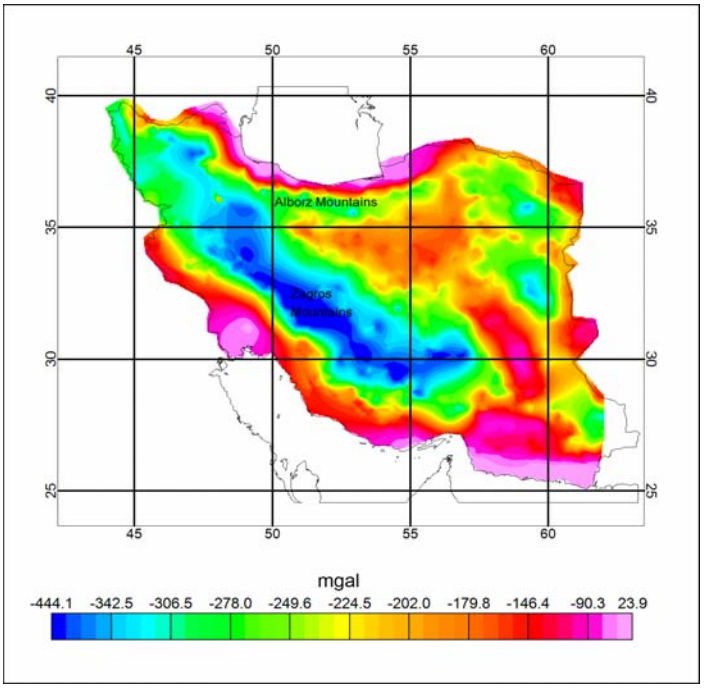

Figure 3. The map of ISOSTA.

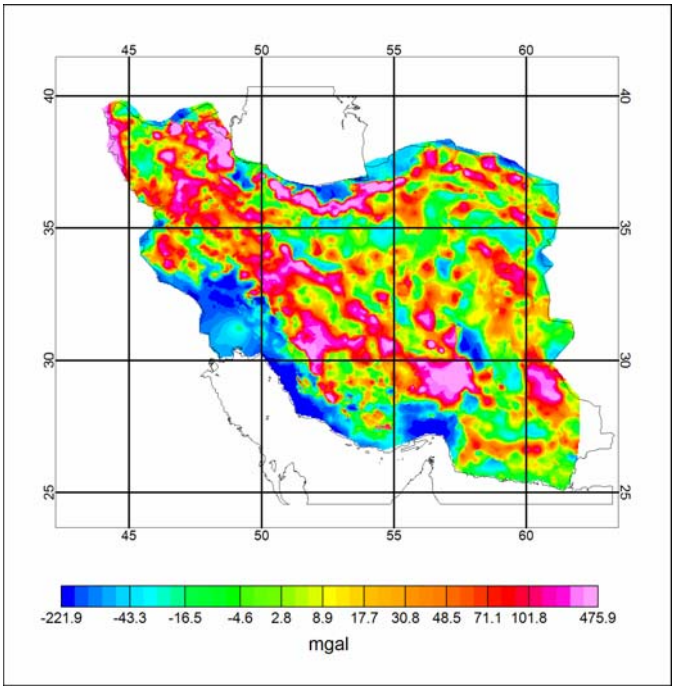

Figure 4. The map of $\delta g^{T}(\text{residual})$, equation (7), in Iran.

There are different techniques for separation of local component from the regional in a gravity anomaly field namely: high pass filtering, low order polynomial fitting, upward continuation (Thurston and Brown, 1992), and using GGMs. In this research we will be using GGMs for the separation.

3.1 GLOBAL GEOPOTENTIAL MODEL APPROXIMATION

Employing a GGM, the residual topographical effect on gravity, $\delta g^{T}(\text{residual})$, is decomposed into its regional and local components:

$$\delta g^{T}(\text{residual}) = \delta g^{T}(\text{regional}) + \delta g^{T}(\text{local}). \quad (8)$$

Newly developed GGMs, e.g., EIGEN-GL04C, seem to be superior to the old GGMs, e.g. EGM96. EIGEN-GL04C is a geopotential model of the Earth, a combined solution, accommodating the satellite GRACE, LAGEOS mission data, $0.5^{\circ} \times 0.5^{\circ}$ mean FA surface gravity anomalies, and the altimetry surface data (http://www.gfz-potsdam.de/pb1/op /grace/ results/). But the new and old models showed almost the same performance in Iran concerning their accuracy in computing the geoid, (Sedighi et al. 2007). The EGM96 model is in the form of a finite series of spherical harmonics complete to degree and order 360, thus, recovering the geoid and gravity anomaly features of wavelengths of 110 km and longer. The model can be used to provide a band of long wavelength free air gravity anomalies up to a harmonic degree selected by a user; of course not exceeding the maximum degree (360) of the model. It can be converted to the same band BAs, using a DTM in addition. For this, the DTM should be first transferred (analyzed) into its spherical harmonic series based on the spherical harmonic functions, (Nahavandchi, 2003). The model is called the Harmonic Topography Model (HTM). The long wavelength part of the HTM transferred to the geopotential coefficients (Vaníček P et al. 1995) is subtracted from the potential coefficients of the selected GGM, yielding the geopotential model corrected for the topographical effect (GGMT). Subtracting the normal (ellipsoidal) potential field (expressed in spherical harmonics) from the GGMT yields the long wavelength potential anomaly field (TGMT) of the Earth in the absence of topography. The gravity anomaly implied by TGMT is then the long wavelength BA. Figure 5 shows the long wavelength BAs derived from the

EGM96 model up to the degree and order of 360. Figure 6 shows the map of EGM96-derived BA-FA. Figure 7 shows the ISOSTA map derived from the EGM96 geopotential model in a similar way to that explained in the previous section. Figure 8 is then the long wavelengths EGM96-derived topographical effect $\delta g^T(\text{long wavelengths})$ up to the wavelength of 110 km or the harmonic degree 360, reduced in accordance with the equations (6) and (7). Figure 9 shows the local topographical effect on gravity, $\delta g^T(\text{local})$, obtained by subtracting the $\delta g^T(\text{long wavelengths})$ from the observed residual topographical effect, $\delta g^T(\text{residual})$, shown in figure 4. The local components in figure 9 contain the short wavelengths ranging from 110 km and shorter (Hackney et al. 2004). According to the relation (1), the local wavelengths belong close to the crustal structures located roughly at a depth of about 20 km to top surface. In other words, the local components contain effects from structures at depths of less than 20 km including the topography.

4 SUBSURFACE DENSITY MAPPING

The local gravity data $\delta g^T(\text{local})$ extracted by the method mentioned above are now an assembly of groups of local data each group representing its own local topography underneath. Hence, the topographical area of each group has to be delimited. According to the longest wavelength available in the data (110 km), the data is divided into groups representing sub-regions of approximately $100\,\text{km} \times 100\text{km}$ area in the region. Considering also the diversity of geological formations, the region of Iran is divided into eight sub-regions of different geological formations shown in figure 10. Based on the locations of boundary lines of the sub-regions the data is dismantled into 8 groups, each group representing its own sub-region. As mentioned in the previous section, for the mapping, one can then go to a depth of 20 km under the surface which is more than the depth of topography needed to be modeled in this research.

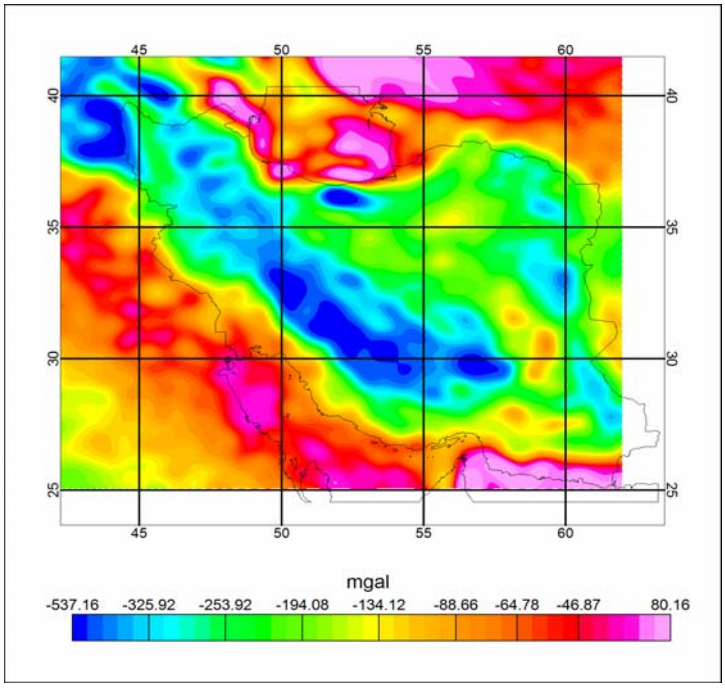

Figure 5. Long wavelengths BA derived from EGM96 model.

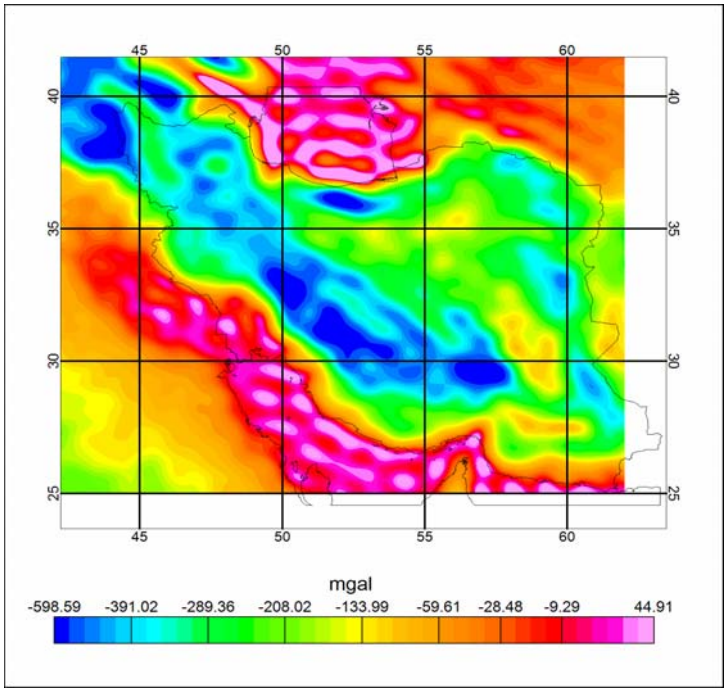

Figure 6. The map of EGM96-derived BA-FA.

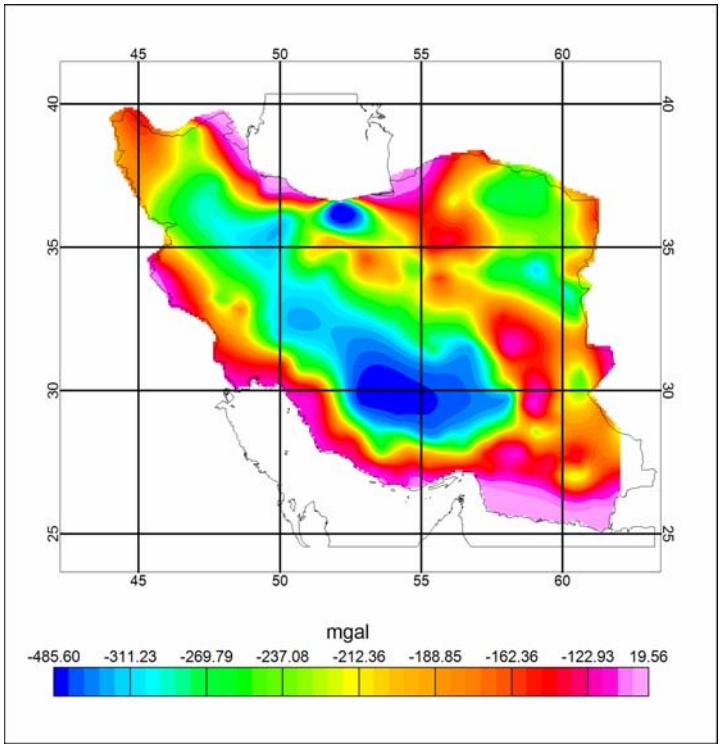

Figure 7. The map of EGM96-derived ISOSTA.

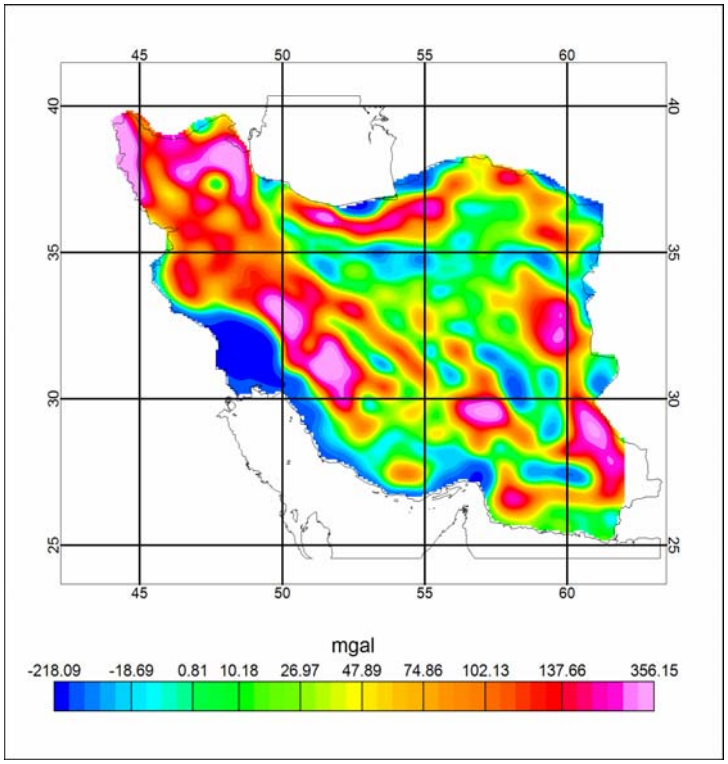

Figure 8. The map of the EGM96-derived δg^{T} (long wavelengths).

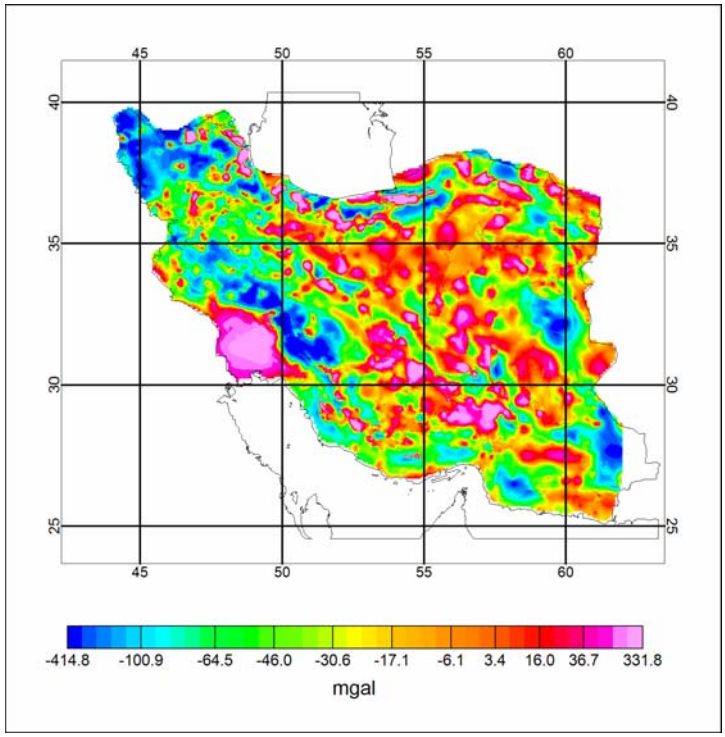

Figure 9. Map of the δg^{T} (local).

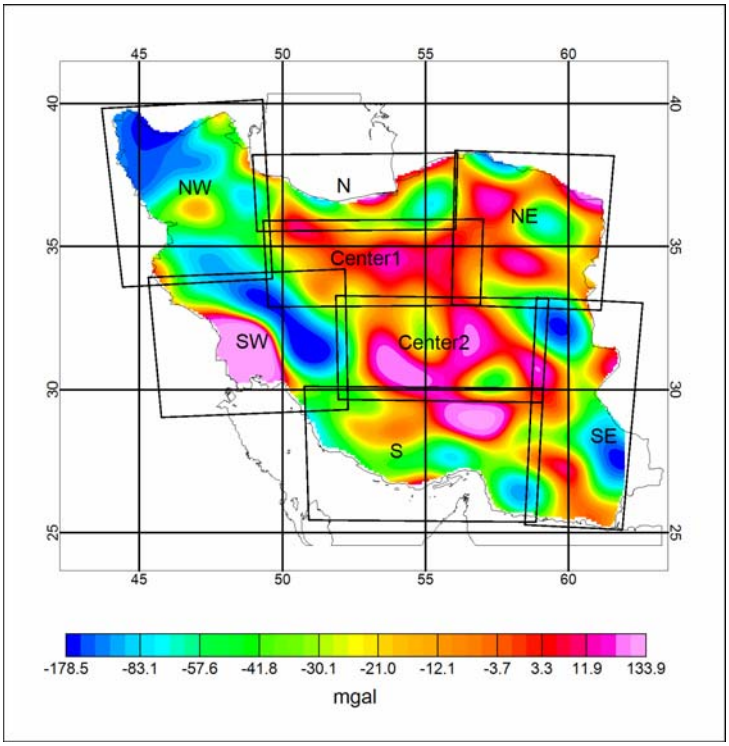

Figure 10. Delimits of the 8 sub-regions in Iran.

For the density modeling of topography underneath a sub-region, the corresponding group of gravity data is first taken to spectral analysis by the method of Power Spectral Analysis (PSA). PSA would provide a reliable basis of information for the techniques estimating the depths of density source bodies. The depth of a source body is related to the slope of the linear segments of the corresponding gravity power spectrum (Najandjock et al. 2006). Figure 11 shows the radially averaged power spectrum of the gravity data in the so called Center1 sub-region shown in figure 10.

There are 4 different slopes recognized in the profile for which the thickness layers are "topography, 1.5 km, 3 km, 11.5 km, 25 km", and the corresponding frequency bands are "high-pass frequency 0.00022, band-pass frequency (0.00022-0.000165), band-pass frequency (0.000165-0.00005), band-pass frequency (0.00005-0.00002) and low-pass frequency 0.00002" respectively. Using the Apparent Density Mapping (ADM) technique (Singh et al. 2003), the lateral mass density distribution of each thickness layer is estimated. For the estimation, an average density proportional to the average depth of the layer considering the depth compact factor is required. Now by the forward modeling (Beck, 1981), the result of ADM for each thickness layer is transformed into its 3-D density model by forward and inverse trial and error attempts until the 3-D model of the thickness layers generates gravity distribution similar to the observed local gravity data within an acceptable error budget. Assembly of the 3-D density models of the thickness layers in one sub-region and assembling of the sub-regions results in a 3-D density model called the 3-D GRAvity implied DENsity (GRADEN) model of the region. Figure 12 shows the GRADEN model of density for the region of Iran. Figure 13 shows the topographical portion of the GRADEN model.

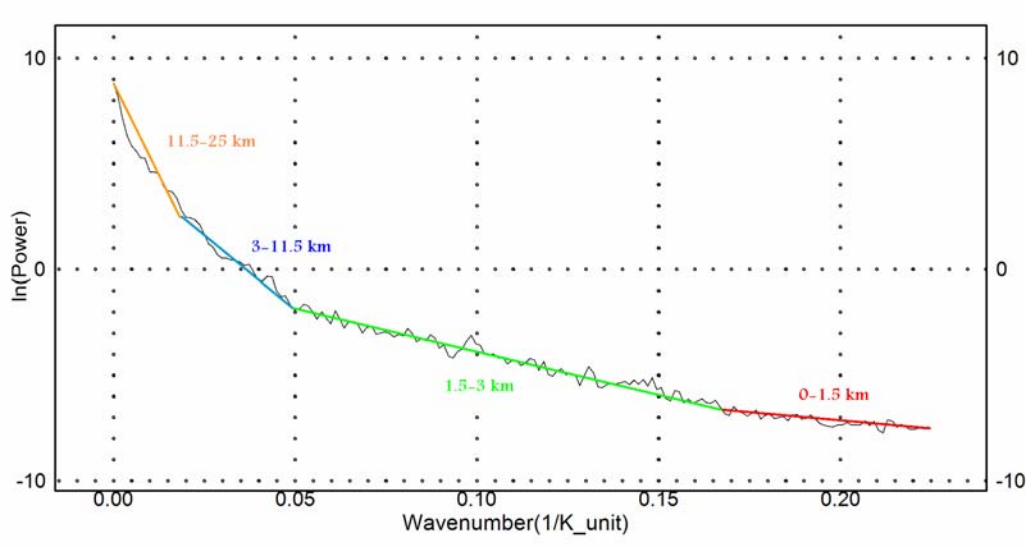

Figure 11. Radially averaged power spectrum of the sub-region called Centerl.

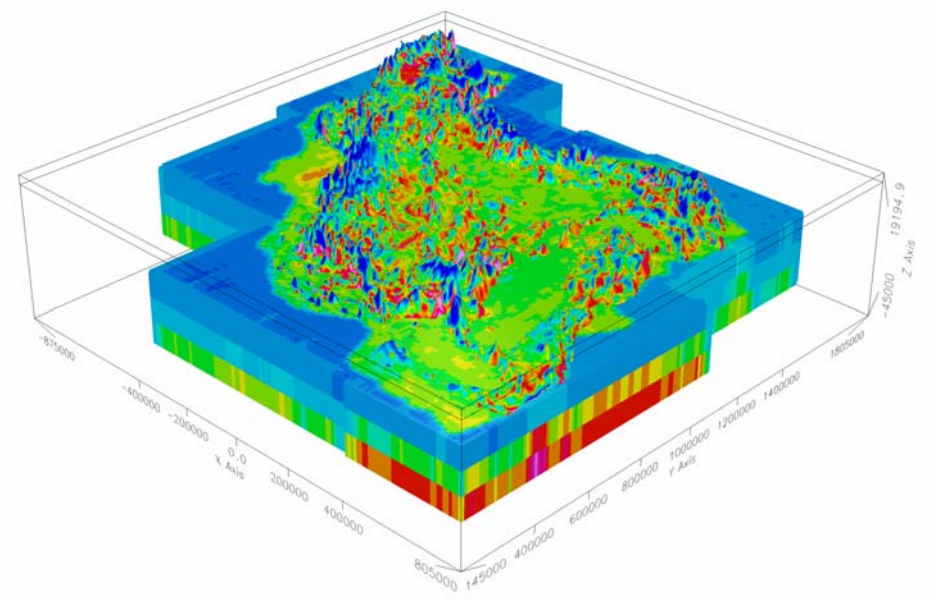

Figure 12. A 3-D GRADEN model of density in Iran.

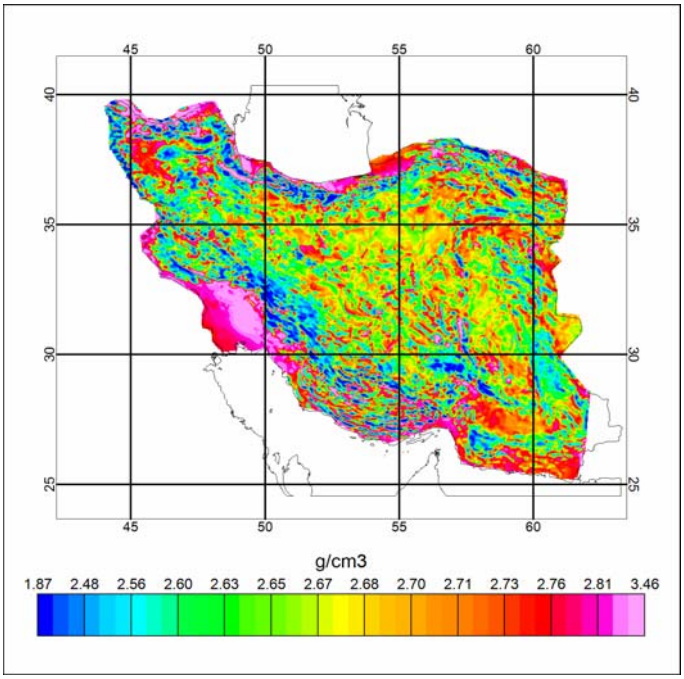

Figure 13. GRADEN model (topographical portion).

5 CONTRIBUTIONS TO THE GEOID

The GRADEN model determined above accommodating the radial and lateral distributions of density into topography is different from the nominal constant density assumption of topography. The difference certainly demonstrates some contribution towards the geoidal height. For the numerical evaluation of the contribution, the Stokes-Helmert geoid software (http://gge.unb.ca/ Research/GRL/ Geodesy Group/) was modified to account for the variable density of topography. In the Stokes-Helmert scheme, the geoid is computed generally in four steps: a) the observed FA on the terrain is transferred to the Helmert space by subtracting DTE (Direct Topographical Effect on gravity) evaluated on the terrain. b) the transferred FA is continued downward to the co-geoid level. In this continuation the SITE (Secondary Indirect Topographical Effect on gravity) is applied. c) the co-geoid is computed by the Stokes integral using the anomalies continued downward onto the co-geoid. d) finally the co-geoid is transformed to the geoid applying the PITE (Primary Indirect Topographical Effect on potential). The effects DTE, SITE, and PITE are computed applying spherical approximation in according to Martinec (1998).

To evaluate the contribution, a "reference" geoid is first computed applying the constant (reference) density of the region equal to $\rho_{\circ} = 2670$ kg.m^{-3}. Figure 15 shows the reference geoid in Iran. Figure 15 shows the contribution of GRADEN minus the constant density.

Numerical statistics of the contributions shown in figure 15 are given in the following table.

6 CONCLUSIONS

The GRADEN map and the information inside could be arbitrarily digitized in point values, provided that the spacing of information of course depends on the spatial distribution of the original observed local gravity data in the region. The 3-D GRADEN model reasonably fits the 2-D GEODEN model in the surface level as it was shown in the sub-region S (figure 14). The GGMs, because of their global characteristics and multiple satellites of various inclinations used in deriving the models, are unbiased in estimating the long wavelength features of the Earth gravity field. Hence, they are reliable in estimating the long wavelength gravity anomalies originated from densities deep sited in the Earth. But the

The statistics of differences between the GRADEN and GEODEN models in geoid.

Difference between the reference and GRADEN geoid models	Min. (m)	Max. (m)	Mean (m)	Standard Deviation (m)
	-1.05	0.56	0.04	0.07

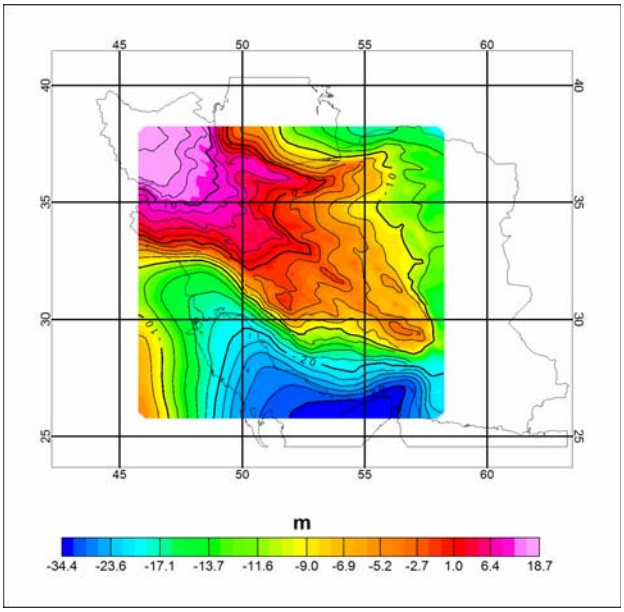

Figure 14. The reference geoid in Iran.

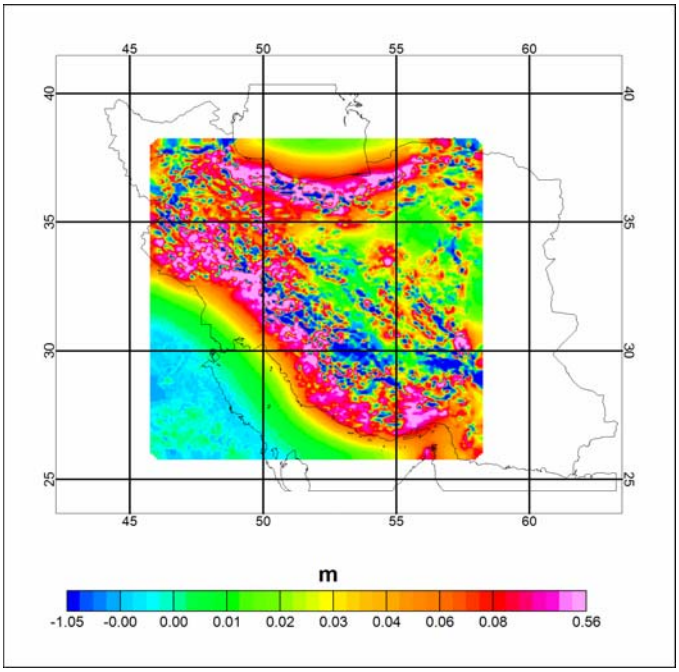

Figure 15. Contribution of the GRADEN model minus the constant density to the geoid in Iran.

harmonic resolution of the GGM models is not enough to extend the estimation of anomalies by a GGM model close to the local or subsurface features. By the GGM of 360 harmonic resolution used, the GRADEN model contains density information beneath the surface to a depth of almost 20 km. In computing the geoid contribution, only the density information of topography in Iran was used in the 3-D integrals of topographical effects. Considering the uncertainty of the GRADEN model which is unavoidable in describing the lateral distribution of density, one may rely on the resolution by Vaníček and Martinec (1994) saying that a knowledge of topographical density variation in the lateral direction good to about 5% is sufficient to compute a geoid accurate to a few centimeters. But the contribution of a GRADEN model itself to the geoid is considerable as shown by figure 15. The contribution on the RMS scale is about 7 centimeters but it may reach up to a few decimeters in few places in the region. They are mountainous places.

REFERENCES

Beck, A. E., 1981, Physical Principles of Exploration Methods. MacMillan, London, p. 73.

Featherstone, W. E., 1997, On the use of the geoid in geophysics: A case study over the north-west shelf of Australia, Explor. Geophys., **28**, 52-57.

Hackney, R. I., Featherstone, W. E., and Gotze, H-J., 2004, Regional–residual gravity field separation in the Central Andes using global geopotential models. ASEG 17th Geophysical Conference and Exhibition, Sydney 2004.

Huang, J., Vaníček, P., Pagiatakis, SD, Brink, W., 2001, Effect of topographical density on geoid in the Canadian Rocky Mountains. J. Geodesy., **74**, 805-815.

Kuhn, M., 2001, Density modelling for geoid determination, Proceedings of GGG2000 IAG International Symposium, Banff, Alberta, Canada, August 2000, pp. 271-276.

Lemoine, FG., Kenyon, SC., Factor, JK., Trimmer, RG., Pavlis, NK., Chinn, DS., Cox, CM., Klosko, SM., Luthcke, SB., Torrence, MH., Wang, YM., Williamson, RG., Pavlis, EG., Rapp, RH., and Olson, TR., 1998, The development of the joint NASA GSFC and NIMA geopotential model EGM96. NASA/TP-1998-206861, NASA, Greenbelt.

Martinec, Z., 1998, Boundary-Value Problems for Gravimetric Determination of a Precise Geoid. Springer-Verlag, Berlin Heidelberg, New York.

Mishra, D.C., Laxman, G., Arora, K., 2004, Large-wavelength gravity anomalies over the Indian continent: Indicators of lithospheric flexure and uplift and subsidence of Indian Peninsular Shield related to isostasy. RESEARCH COMMUNICATIONS-CURRENT SCIENCE, **86**, 861-867.

Nahavandchi, H., 2003, A comparison of different procedures of handling the effects of close and distant topographic masses in gravimetric geoid computations with the classical and recent formulae. Newton's Bulletin-n°1, Dec. 2003-ISSN 1810-8555.

Najandjock, N. P., Manguelle-Dicoum, E., Ndougsa-Mbarga, T., and Tabod, C. T., 2006, Spectral analysis and gravity modeling in the Yagoua, Cameroon, sedimentary basin. Geofis. Int., **45**(2), 209-215.

Sedighi, M., Najafi Alamdari, M., Djamour, Y., and Nankali, H. R., 2007, Comparison of geopotential models-A case study in Iran, EGU2007-A-02142; G3-1WE5P-0344.

Singh, AP., Mishra, DC., Laxman, G., 2003, Apparent Density Mapping and 3-D Gravity Inversion of Dharwar Crustal Province. J. Ind. Geophys. Un., **7**, 1-9.

Subba, Rao, DV., 1996, Resolving Bouguer anomalies in continents-A new approach. Geophys. Res. Lett., **23**, 3543-3546

Thurston, J. B., and Brown, R. J., 1992, The Filtering Characteristics of Least-squares Polynomial Approximation for Regional/Residual Separation. Canadian J. Exp. Geophys., **28**, 71-80.

Tziavos, IN., and Featherstone, WE., 2001, First results of using digital density data in gravimetric geoid computation in Australia., in Sideris MG (ED), Gravity, Geoid and Geodynamics, Springer, Berlin, pp. 335-340.

Tziavos, IN., Sideris, MG., and Sünkel, H., 1996, The effect of surface density variations on terrain modelling-a case study in Austria. Report 96.2, Finnish Geodetic Institute, 99-110.

Vaníček, P., and Martinec, Z., 1994, The Stokes-Helmert scheme for the evaluation of a precise geoid, Manuscr. Geodaet., **19**, 119-128.

Vaníček, P., Najafi, M., Martinec, Z., Harrie, L., and Sjöberg, LE., 1995, Higher degree reference field in the generalized Stokes-Helmert scheme for geoid computation. J. Geodesy., **70**, 176-182.

Vaníček, P., Huang, J., Novak, P., Veronneau, M., Martinec, Z., and Featherstone, W. E., 1999, Determination of the boundary values for Stokes-Helmert problem. J. Geodesy., **73**, 180-192.